Parametrization and model validation for metal using J2 Plasticity and digital image correlation

V. Chandra[1]
P. Chakraborty[1]

Abstract

Conventionally, the parameters of elasto-plastic material models are calibrated using experiments that develop homogeneous strain/stress fields, while the model is then used in applications where the responses are heterogeneous in nature depending on the structural geometry and/or nature of loading. This entails that the local response predicted by a considered model should also be validated with experiments that develop heterogeneous and multiaxial strain/stress fields. In the present work, the adequacy of the widely used von Mises elasto-plastic model for a 6000 series Aluminium alloy is explored under this general idea. The model parameters are first calibrated from uniaxial tension test using digital image correlation (DIC). The predictability of the considered model is then evaluated for a uniaxially pulled plate with a center hole that develops a heterogeneous strain field. Finite Element Method simulation is performed to numerically predict the strain distribution, which is then compared with the strain field measured using Digital Image Correlation (DIC).

Keywords: *J_2 Plasticity, Digital image correlation (DIC), Calibration and Validation, Aluminum alloy.*

[1] *Department of Aerospace Engineering, India Institute of Technology, Kanpur, Uttar-Pradesh, 208016.*

Introduction

Aluminium alloys have been used for making main airframe due to their desirable specific properties. These are their low density, cost and ease of fabrication. Drawbacks of Aluminium alloys include relatively low modulus of elasticity when compared to other metals, susceptibility to corrosion and low elevated-temperature capability (Campbell, 2006). While pure Aluminium has extremely low strength, it can be significantly improved by mixing with other elements to form its alloys (Rana et al.,2012; Medrano-Prieto et al., 2016; Zhang at al., 2016). Multistage ageing treatments are also used to further improve the properties of the alloy systems (Polmear at al., 2004). These high strength and lightweight Aluminium alloys are thus extensively used, especially in the aerospace and automotive industry, for structural applications considering weight saving along with low cost. In aerospace industry, structural components such as in the CC-130 Hercules transport aircraft and the Canadian Air Force CP-140 Aurora maritime patrol aircraft widely uses Aluminium alloy (Chlistovsky et al., 2007).

Proper material selection is one of the important aspect of engineering design. However, detailed characterization and accurate model of deformation behavior of a material should also be available to make a judicious choice. These applies to Aluminium alloys as well. With the advent of novel characterization methods and analysis techniques, improvements in the models describing the deformation behavior of these alloys are continuously being made. For example, artificial neural network approach has been applied in Al-Khedher et al. (Al-Khedher et al., 2006), to accurately model the behavior of age hardened Aluminium alloys. Such models can be extremely useful to predict structural behavior of aerospace structures with geometrical imperfections and enable more rigorous design optimization with stricter constraints.

In the realm of material models for Aluminium and other metallic alloys, development of appropriate constitutive relations capturing their elasto-plastic behavior have received significant attention in the past and is also an area of continual research. A detailed review on such constitutive theories of plasticity for metallic alloys can be found in Chaboche (Chaboche., 2008). While a vast number of anisotropic and asymmetric models describing the elasto-plastic behavior of metallic systems have evolved over the years, the J_2 plasticity theory remains the most commonly used and has been implemented in several finite element codes. As discussed by several authors (Fredriksson et al., 2009; Ihsan., 1998; Moreira et al., 2007; Argyris et al., 1984), it is assumed in the J_2 plasticity theory that material yielding and flow stress are driven by the second invariant of the deviatoric stress tensor only. The model has been found to predict the elasto-plastic response of various metals and alloys in the low- medium plastic rang with sufficiently good correlation with experimental outcomes. However, the model is deficient in capturing the experimentally observed behavior for in the full domain of elasto-plasticity (Taylor et al., 1932; Spitzig et al., 1975).

Parameterization and validation of J_2 elasto-plastic model require experimental evaluation of properties such as Young's modulus, Poisson's ratio and elasto-plastic profile of a material. The most common method for finding the material properties is strain gage based extensometer but is limited by the applicable strain range. Several researchers have proposed the 2D-Digital image correlation (DIC) for elasto-plastic property evaluation with the advantage that it can be used for the entire range of applied strain accurately. Furthermore, the method than can be used for obtaining the in-plane displacements and strains at a local level (Sutton et al., 2009). DIC is a full-field non-contact optical method that obtains displacement and strain fields from acquired images. The calculations are based on random speckles decorated on the specimen surface and translate during specimen deformation.

The basic principle of DIC is the tracking of the same image points by comparing the grey level pixel values located in the two digital images of the test specimen

surface recorded before (reference) and after deformation (current). The tracking is done by search for extremum correlation in a deformed and undeformed state. Test specimen surface must be covered with a random speckle pattern, which deforms together with the specimen surface as a carrier of deformation information. DIC was first developed by a group of researchers at the University of South Carolina in the 1980s (Pan et al., 2009; Bruck et al., 1989; Sutton et al., 1983). The method has been applied successfully to calculate the full field displacement and strain fields for homogeneous and inhomogeneous deformation (Pan et al., 2007).

Experimental Procedure

Specimen material and geometry

The standard specimens of 6063-T6 aluminum alloy (chemical composition of 6063T6 aluminum alloy is summarized in Table 1) were designed and machined according to ASTM standard E8/E8M-13a from single extruded bar having cross section of 76.20 × 16 mm, as shown in figure 1. In the figure, G is the gauge length, W is the width of the gauge section, T is the thickness of the specimen, R is the radius of the fillet between gauge section and the grip section, B and C are the lengths and widths of the grip section, respectively, L is the overall (total) length, and D is diameter of hole. Dimensions (in mm) of different specimens used in the experimental program are presented in table 2. Two kinds of specimens were used; one with and the other without a central hole. Specimen were properly polished in the gage section and hatched in the grip section prior to testing in order to enhance the reliability of the test data.

Table1: Chemical compositions of 6063T6 Aluminum alloy.

Component	Si	Fe	Zn	Mg	Sn	Ti	V	Pb	Ni	Cr	Al
Wt (%)	0.469	0.178	0.035	0.656	0.069	0.025	0.013	0.080	0.086	0.008	98.369

Figure 1

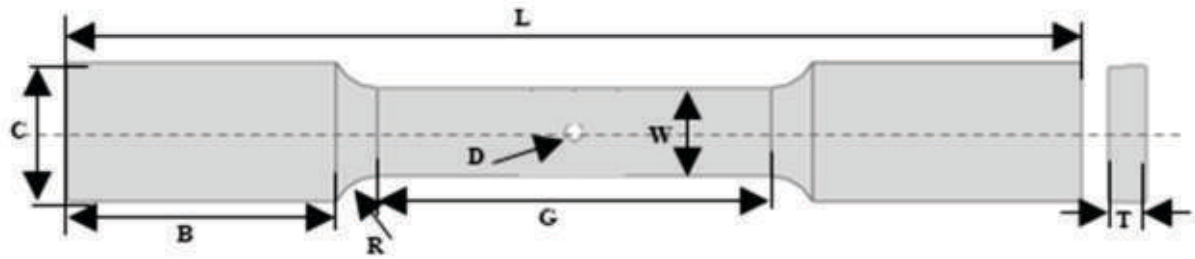

Geometry of a typical dog-bone shaped specimen (ASTM standard E8/E8M-13a).

Table 2: Geometric Parameters of both the specimens.

Parameter (mm):	G	W	T	R	B	C	L	D
Specimen without Hole:	57	12.68	3.92	6.76	39	20	147	N.A.
Specimen with Hole:	57	12.68	3.92	6.76	39	20	147	2.25

Speckle pattern

In DIC the specimen surface must be decorated with random grey intensity distribution known as speckle pattern. These speckle pattern may be naturally present or have to be artificially created (Pan et al., 2009; Dong et al., 2017). The speckle pattern should have largely varying gray scale intensity gradients, non-periodic and non-repetitive pattern without directionality, to ensure accurate DIC measurements. Size of speckle granules of 3–5 pixels or greater are recommended to avoid aliasing effect. These speckle patterns are carrier of deformation information and deform together with the specimen surface. So, it is necessary to create sufficiently strong speckle pattern with good interface strength. Speckle pattern layer must also be sufficiently to disallow a thickness effect on its deformation (Reu., 2014; Reu., 2015; Reu., 2015; Reu., 2014)

The process of making artificial speckle patterns starts with applying a very thin and flat layer using white aerosol paint. Once surface get dry, spraying black paint to produce fine dots on pre painted surface from appropriate distance to get optimal size of speckle granules. Images of speckle patterns as shown in figure 2.

Figure 2: Speckled Specimen, (a) Dog-bone shaped specimen without central hole, (b) Dog-bone shaped specimen with central hole.

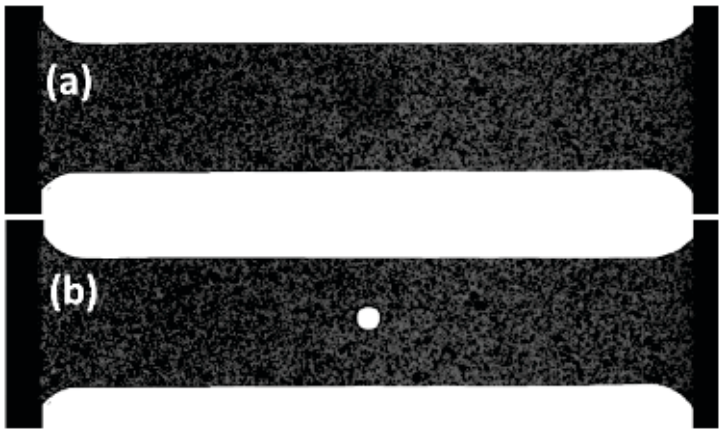

Tensile Testing

Tensile tests were conducted using 15 kN capacity screw driven INSTRON Universal Testing Machine (UTM) equipped with a DIC setup consisting of a camera and led lamps as shown in figure 3. The tensile testing was performed at a displacement rate of 0.5 mm/min. The digital camera records the 2D projection of specimen's surface. Hence, the optical axis of the digital camera was kept perpendicular to the specimen's surface. Post processing of the captured images was done using VIC-2D software. Speckled specimens tested on this setup and after fracture are shown in figure 4.

Figure 3: Experimental Setup: UTM Equipped with Camera and lamps for DIC

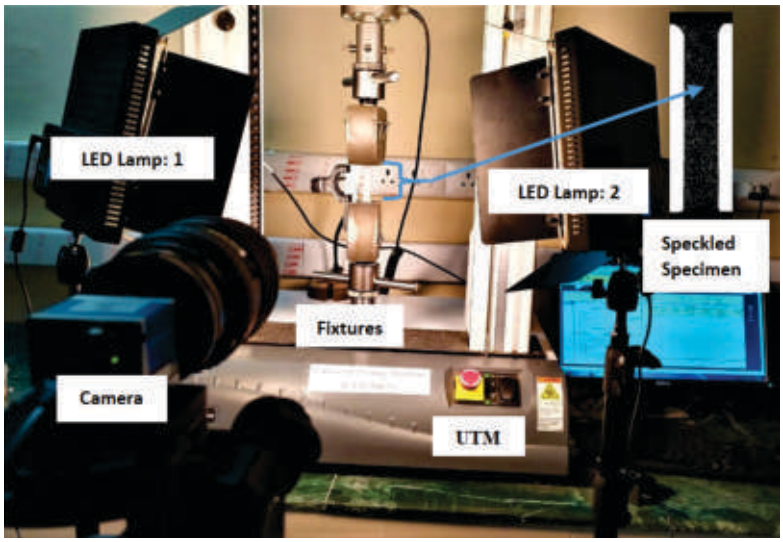

Figure 4: Broken Dog-bone Shaped Specimens: (a) without and (b) with central hole.

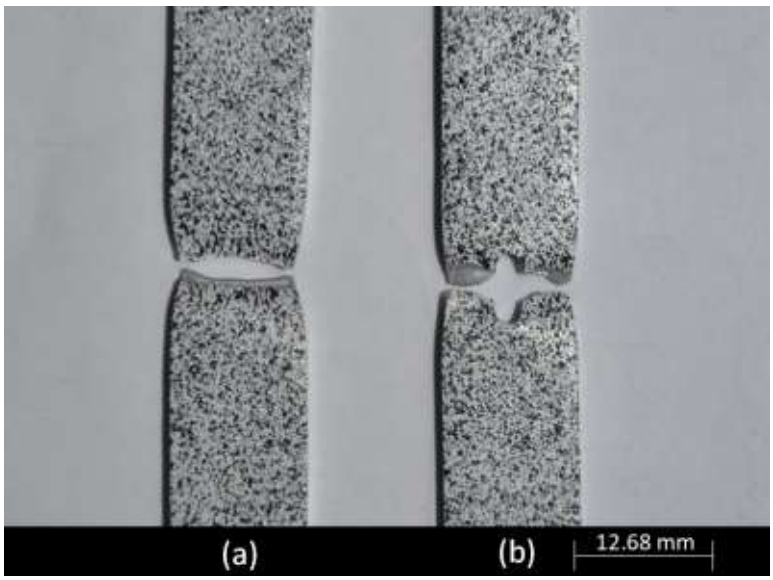

DIC for Strain Measurement

DIC technique consists of three steps, namely (a) creating random speckles to produce grey intensity imaging features on specimen surface; (b) capturing the digital image of the undeformed specimen and at different stages of deformation during testing; and (c) post processing of captured images using appropriate DIC algorithm to calculate full-field displacement and its gradients. In order to perform DIC post-processing, an area for analysis called region of interest (ROI) is marked and it is sub divided into evenly spaced virtual grids after recording of the images. Displacements and its gradients are calculated at each point of these virtual grids. The marked black square, shown in figure 5a, encloses a group of pixels and is called a subset. Subsets are identified to track the same point, usually their center points, from the images of the specimen before and after deformation image. The tracking points before and after deformation, labelled as $\boldsymbol{P}(x_0, y_0)$ and $\boldsymbol{P}'(x_0', y_0')$ are shown in figure 5b.

Figure 5: Basic principle of subset based DIC method. (a) post-processing parameters, (b) correlation of subset from reference image to deformed image.

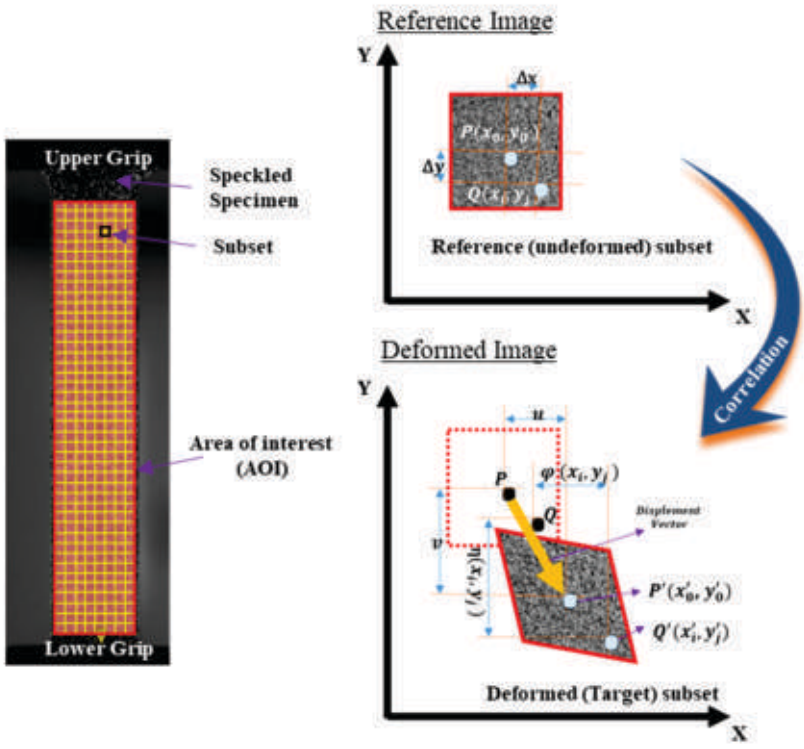

(a) (b)

To ensure uniqueness condition of image features, it is recommended not to consider single pixel as calculation point because there could be the possibility of more than one pixel having same intensity value in selected region of interest (ROI), hence a group of (2M+1) ×(2M+1) pixels is considering as subset of square shape as shown in figure 5b. The Square shape of subset changes in the deformed image due to deformation in test specimen. The point $\boldsymbol{Q}(x_i, y_j)$ near the center of subset point $\boldsymbol{P}(x_0, y_0)$ in undeformed subset can be mapped to the point $\boldsymbol{Q}'(x_i', y_j')$ in deformed subset having center point $\boldsymbol{P}'(x_0', y_0')$ as shown in figure 5b. The displacement mapping function is defined by:

$$x_i' = x_i + \varphi(x_i, y_j) = x_0 + \Delta x + \varphi(x_0 + \Delta x, y_0 + \Delta y)$$

$$y_j' = y_j + \eta(x_i, y_j) = y_0 + \Delta y + \eta(x_0 + \Delta x, y_0 + \Delta y)$$

where ϕ and η are the shape function. Second order shape function are applicable for very large strains. There are also accurate to capture deformation shapes such as rigid body rotation, pure shear, uniaxial and biaxial tension etc. of the subset. The shape function chosen here is

$$\varphi(x_i, y_j) = u + u_x \Delta x + u_y \Delta y + \frac{1}{2} u_{xx}^2 \Delta x^2 + \frac{1}{2} u_{yy}^2 \Delta x^2 + u_{xy}^2 \Delta x \Delta y$$

$$\eta(x_i, y_j) = v + v_x \Delta x + v_y \Delta y + \frac{1}{2} v_{xx}^2 \Delta x^2 + \frac{1}{2} v_{yy}^2 \Delta x^2 + v_{xy}^2 \Delta x \Delta y$$

where $\Delta x = x_i - x_0$, $\Delta y = y_j - y_0$, u and v are the x and y directional displacement components of the reference subset centre, respectively. $u_x\ u_y\ v_x\ v_y$ are the first order and $u_{xx}\ u_{yy}\ u_{xy}\ v_{xx}\ v_{yy}\ v_{xy}$ are second order displacement gradients of the reference subset.

The tracking of subset is evaluated using appropriate correlation functions which can be either cross-correlation (CC) or sum of squared difference (SSD). More recent correlation criterion such as Zero-Normalized Sum of Squared Difference (ZNSSD) (Pan et al., 2009; Pan et al., 2007) are now available.

Zero-Normalized Sum of Squared Difference (ZNSSD):

To evaluate the similarity condition between the undeformed and deformed subset a correlation criterion should be considered. For finding the deformation of subset the correlation criterion should be find its extremum value. Zero-Normalized Sum of Squared Difference (ZNSSD) is one of the correlation criteria and can be written in the form:

$$C_{ZNSSD} = \sum_{i=-M}^{M}\sum_{j=-M}^{M}\left[\frac{f(x_i,y_j)-f_m}{\Delta f} - \frac{g(x_i',y_j')-g_m}{\Delta g}\right]^2$$

where $f(x_i,y_j)$, $g(x_i',y_j')$ are the undeformed and deformed grey intensity function respectively, f_m, g_m are the undeformed and deformed mean grey intensity function respectively are defined as

$$f_m = \frac{1}{(2M+1)^2}\sum_{i=-M}^{M}\sum_{j=-M}^{M} f(x_i,y_j)$$

and

$$g_m = \frac{1}{(2M+1)^2}\sum_{i=-M}^{M}\sum_{j=-M}^{M} g(x_i',y_j')$$

and Δf, Δg are the undeformed and deformed standard deviation grey intensity function respectively given by

$$\Delta f = \sqrt{\sum_{i=-M}^{M}\sum_{j=-M}^{M}[f(x_i,y_j)-f_m]^2}$$

and

$$\Delta g = \sqrt{\sum_{i=-M}^{M}\sum_{j=-M}^{M}[g(x_i',y_j')-g_m]^2}$$

Subsequently, the strain field can be computed after smoothing and differentiating the displacement field (Pan et al., 2007; Pan et al., 2009). Once the displacement gradients are obtained, the Lagrangian strain can be evaluated following:

$$E_{ij} = \frac{1}{2}\left[\frac{\partial u_i}{\partial x_j} + \frac{\partial u_j}{\partial x_i} + \sum_{k=1}^{2}\frac{\partial u_k}{\partial x_i}\frac{\partial u_k}{\partial x_j}\right]$$

Accuracy of DIC results depends on many factors. These can be related to:

(I) Speckle pattern like size, shape, density, contrast and illumination.

(ii) Digital camera features such as resolution, dynamic range, noise, type of lens and frame rate.

(iii) Post-processing features such as interpolation, correlation criterion, shape function, subset size and subset overlap etc.

For accurate results these parameters need to be optimized for the respective application (Acciaioli et al., 2008).

Calibration of DIC System

As the specimen size is large enough to use any contact type strain measurement techniques, a mechanical extensometer was used in this work to measure the global strain from uniaxial tensile testing. These global strains were used for calibration of DIC system using dog-bone specimen under tensile loading. The crosshead displacement of UTM is usually larger than extensometer data due to excess compliance of the test system. Thus, the measured crosshead displacement was compliance corrected before comparing with the extensometer and DIC results. The load displacement curves using the compliance corrected crosshead displacement, extensometer and DIC data are compared in figure 6.

Figure 6: Comparison of load displacement curves between crosshead, DIC system, mechanical extensometer and compliance corrected crosshead displacement.

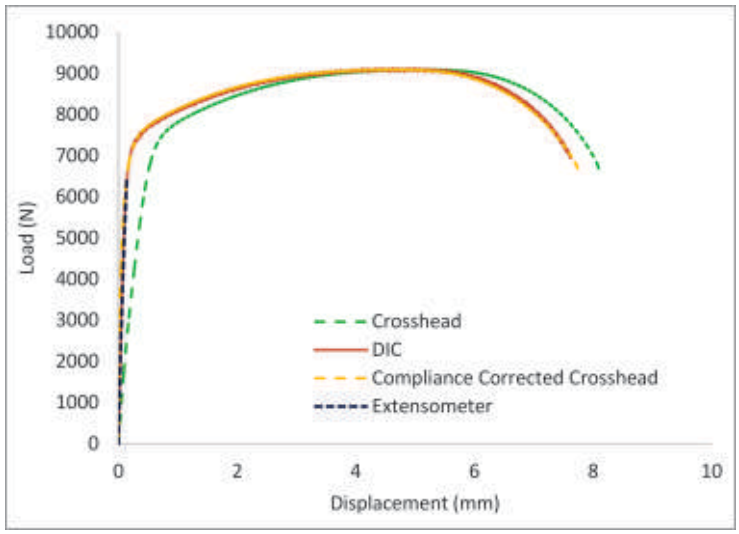

Numerical simulation

Parameterization and validation of J_2 plasticity model requires material properties like Young's modulus, Poisson's ratio and hardening curve. To define material behavior in numerical simulation, basic material properties required are obtained from stress–strain relations which are generally obtained from the uniaxial tensile test of a dog-bone specimen. True stress-strain data is obtained from the corresponding engineering stress-strain data and is shown in figure 7. The parametrization is an iterative process and the following parameters were obtained after several iterations:

Young's modulus of 68.824 GPa, Poisson's ratio of 0.33, yield strength of 142 MPa, and a hardening profile as shown in figure 8.

Figure 7: Calculation of True stress-strain from Engineering stress-strain data.

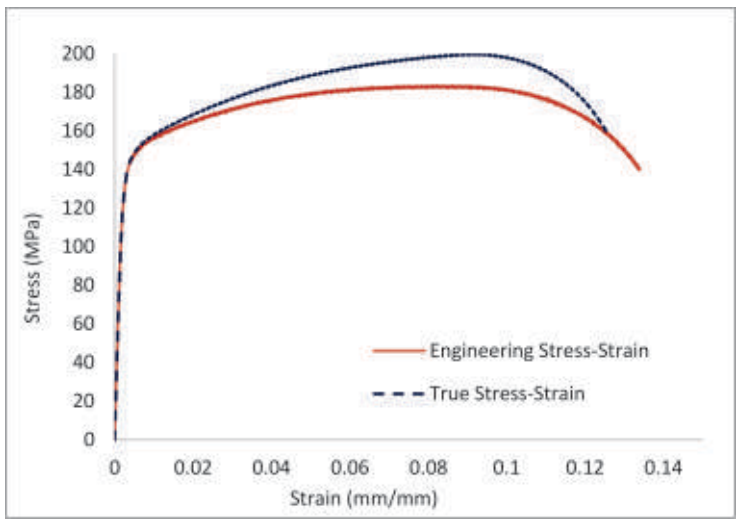

Figure 8: Elasto-Plastic Hardening Curve (input as material model parameter).

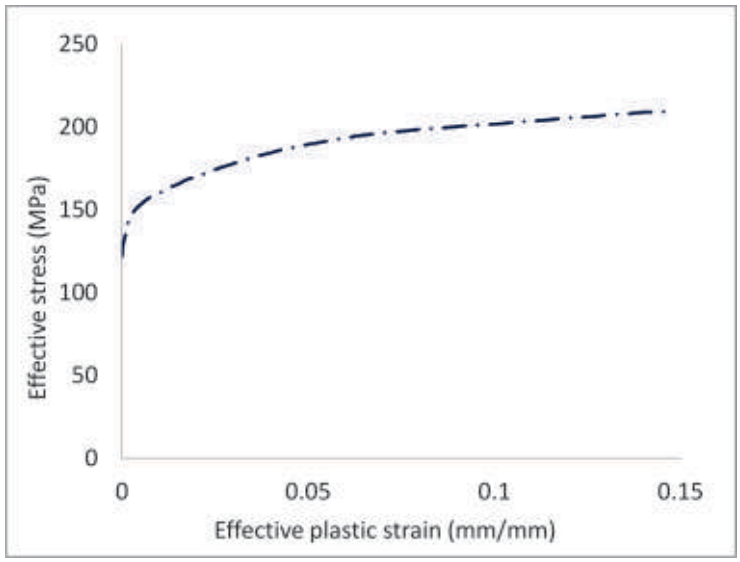

For model parametrization, elasto-plastic Finite Element Method (FEM) analysis of specimen without hole was performed using a commercial package (ABAQUS, C., 2017). C3D8R 8-node trilinear elements, reduced integration and hourglass control were used. 3D model of full specimen geometry was utilized to minimize the effect of approximation on strain localization. The simulated geometry and boundary conditions were similar to the experimental tensile tests and are shown in figure 9(a). The simulated full field strain field is shown in figure 9(b).

Figure 9: Boundary conditions and (b) simulated strain field for Dog-bone shaped specimen without central hole.

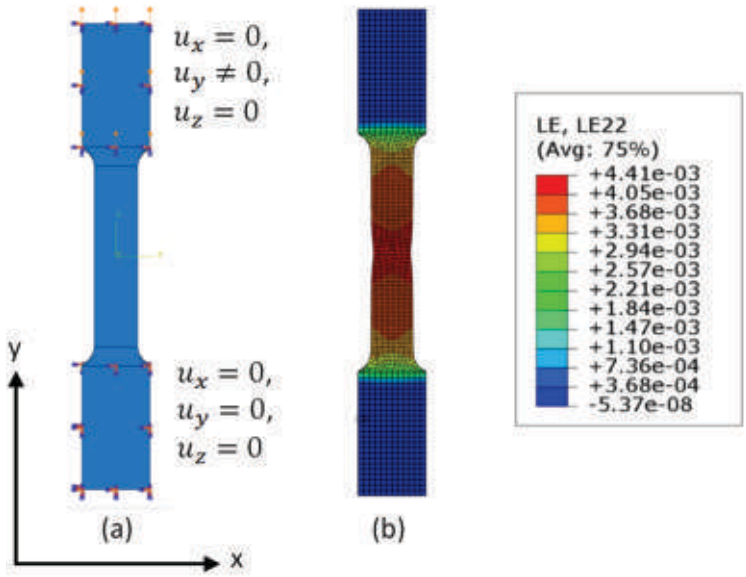

The comparison of stress-strain curves between simulation and experiments after calibration are shown in figure 10. The stress from simulation in figure 10 are calculated from the sum of reactive forces on the nodes in the grip divided by the gauge original area, while the strain is calculated from the average displacements of the nodes on the top and bottom edges of the gauge section. From figure 10, an excellent agreement can be seen starting from elastic regime to yielding followed by strain hardening and initial softening due to neck formation. A mismatch can be observed only near to the final failure of the specimen. The iteratively obtained strain hardening curve shown in figure 8 clearly demonstrates the presence of a very short stage II and a relatively dominant stage III hardening. This behavior is observable in most of the Alumimium alloys. The accuracy of our simulated response can be attributed to the precision of this strain hardening curve. The strain softening observed in the engineering stress strain curves is due to the necking phenomenon.

Figure 10: Comparison of stress vs strain response between experiments and simulations for the plate without central hole.

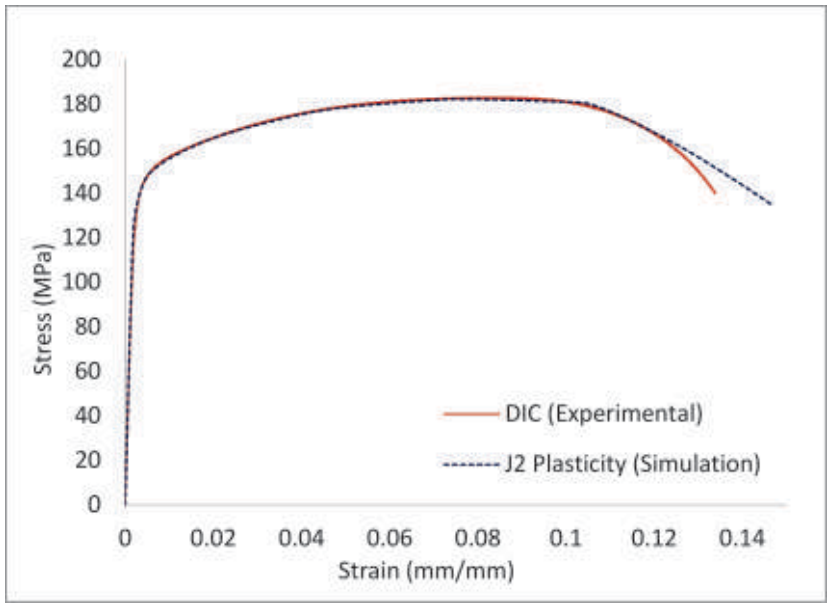

Results and discussion

Validation of the J2 plasticity model for a heterogeneous scenario was performed using the dogbone specimen with a central hole shown in figure 11. In this problem, every point on the plate acts as a virtual extensometer in the DIC technique and experiences a locally multiaxial stress field, particularly near the hole, though the globally applied load is uniaxial. Hence, the comparison of the simulated field with the full-field solution of DIC can also be considered to be a validation of the model under locally multiaxial states. The calibrated constitutive model was used and simulated with similar geometry and boundary conditions as of experiments. The simulated strain field at stress level of 106.94 MPa is shown in figure 11.

Figure 11: Boundary conditions and simulated strain field for Dog-bone shaped specimen with central hole.

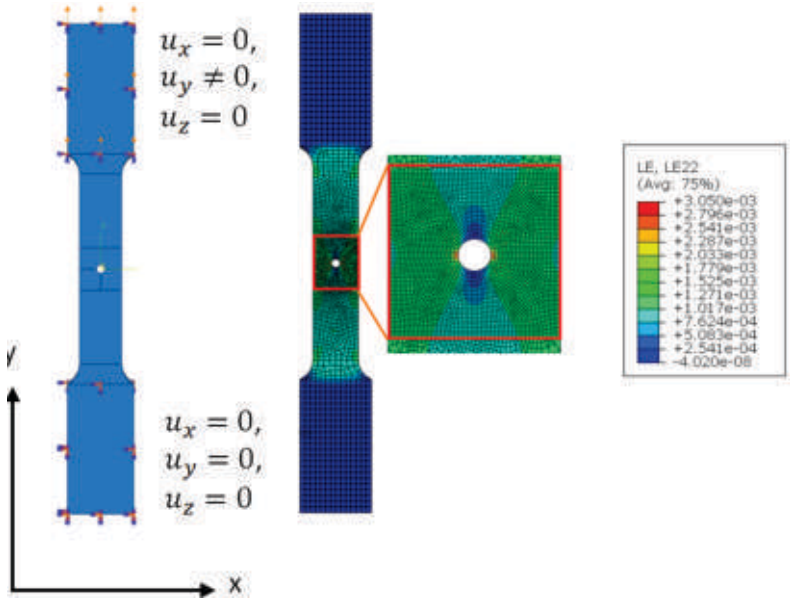

Global load-displacement and stress-strain behavior are presented in figures 12 and 13 to show the fidelity of J_2 plasticity model. The load-displacement results are matching well till maximum strength of material as can be seen from figure 12.

Figure 12: Comparison of load vs displacement response between experiments and Simulations for the plate with central hole.

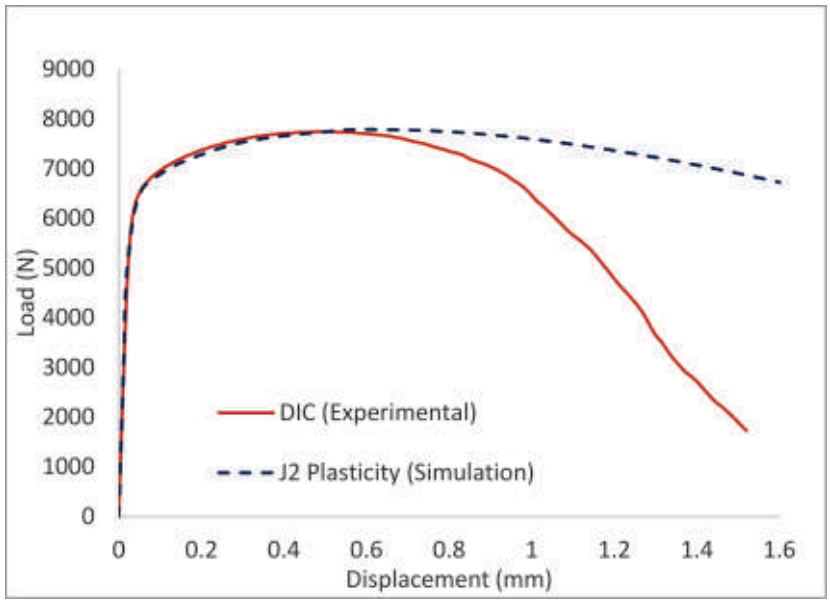

Figure 13: Comparison of stress vs strain response between experiments and Simulations for the plate with central hole.

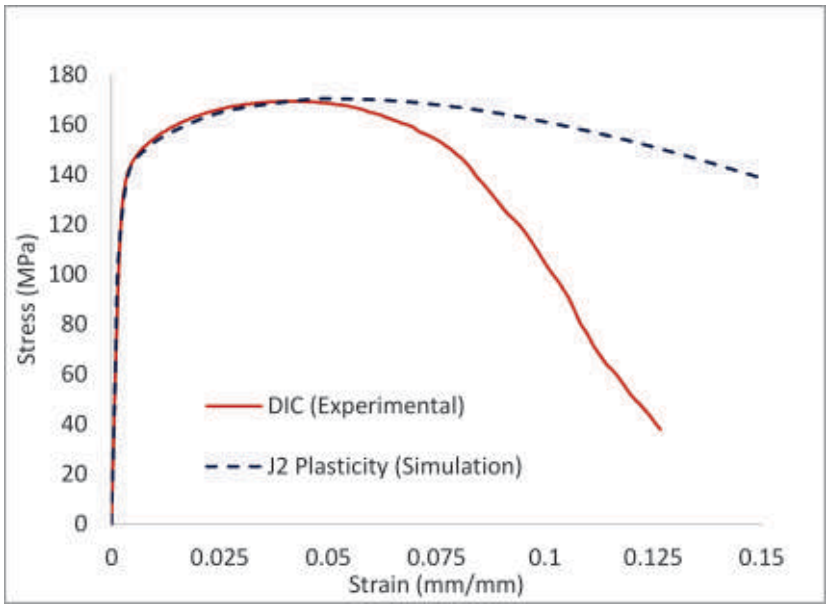

The heterogeneous strain field in the plate with a hole under uniaxial tension is compared between DIC and FEM simulations to validate the accuracy of the model. This comparison is done at a macroscopic stress level of 106.94 Mpa. Furthermore, the strain values along a horizontal line passing through the center of hole was considered for comparison. These comparisons are shown in figure 14. From both the contour and line comparisons it was seen that the J_2 elasto-plastic model can capture the multiaxial response with reasonable accuracy.

Figure 14: Comparison of Variation of local strain between experiments and Simulations for dog-bone shaped tensile specimen with central along horizontal line (at Stress Level of 106.94 MPa).

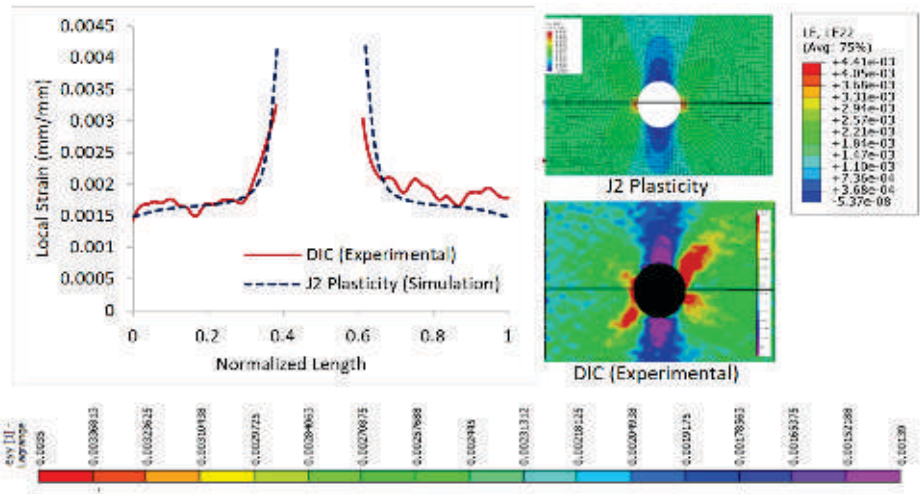

Conclusion

A combined DIC and FEM simulation-based study was performed in this work to explore the accuracy of the J_2 plasticity model when applied to heterogeneous and multiaxial scenario. The parameters of the model such as Young's modulus, Poisson's ratio and elastoplastic hardening profile of material were calibrated using experimental tests that developed homogeneous strain/stress fields. The calibration strategy involved an iterative procedure of simulation and comparison with experimental data till a reasonable match was obtained.

FEM simulations and DIC has been used to evaluate the fidelity of the isotropic von Mises elasto-plastic model for 6063T6 aluminum alloy for both homogeneous, heterogeneous and multiaxial scenario. The comparison of global and full field response between FEM simulations and experiments show that the model reasonably captures the multiaxial constitutive behaviour of the material prior to necking. Appropriate damage model needs to be included to model the response of the material till failure.

References

- ABAQUS, C. (2017). Analysis user's manual.
- Acciaioli, A., Lionello, G., & Baleani, M. (2008). Experimentally Achievable Accuracy Using a Digital Image Correlation Technique in measuring Small-Magnitude (<0.1%) Homogeneous Strain Fields. *Materials (Basel)*, 11(5), 751.
- Al-Khedher, M. A., Yassar, R. S., & Pezeshki, C., & Field, D. P. (2006). A novel structural-based approach to model the age hardening behaviour of aluminium alloys. Modelling Simul. Mater. Sci. Eng. 14, 905–921. DOI: DOI: http://dx.doi.org/10.1088/0965-0393/14/6/002
- Argyris, J.H., Kleiber, M. (1984). Finite Elements in Non-Associated Plasticity-Axisymmetric Necking in Void-Containing Materials. Computer Methods in Applied *Mechanics and Engineering*, 43, 325-347, North-Holland.
- ASTM E8/E8M - 13a Standard Test Methods for Tension Testing of Metallic Materials.
- Bruck, H. A., McNeill, S. R., Sutton, M. A., & Peters III, W. H. (1989). Digital image correlation using Newton-Raphson method of partial differential correction, E*xperimental Mechanics* volume 29, 261-267
- Campbell, F. C. (2006). Manufacturing technology for aerospace structural materials. *Butterworth-Heinemann Publication*, New York, NY, USA.
- Chaboche, J.L. (2008). A review of some plasticity and viscoplasticity constitutive theories. *International Journal of Plasticity*, 24, 1642–1693.
- Chlistovsky, R.M., Heffernan, P.J., & DuQuesnay, D.L. (2007). Corrosion-fatigue behaviour of 7075-T651 aluminum alloy subjected to periodic overloads. International Journal of Fatigue 29, 1941–1949.
- Dong, Y.L., Pan, B. (2017). A Review of Speckle Pattern Fabrication and Assessment for Digital Image Correlation. *Experimental Mechanics*, 57,1161-1181.
- Ihsan, A. K. (1998). A Plasticity Theory and Finite Element Implementation of Friction model. *Jurnal Kejuruteraan*, 10, 51-62.
- Medrano-Prieto, H. M., Garay-Reyes, C. G., Gómez-Esparza, C. D., Aguilar-Santillán, J., Maldonado-Orozco, M. C., & Martínez-Sánchez, R. (2016). Evolution of Microstructure in Al-Si-Cu System Modified with a Transition Element Addition and its Effect on Hardness, *Mat. Res., 19, 1.* DOI: http://dx.doi.org/10.1590/1980-5373-MR-2015-0673
- Moreira, L. P., Ferron, G. (2007). Finite element implementation of an orthotropic plasticity model for sheet metal forming simulations. *Latin American Journal of Solids and Structures*, 4, 149–176.
- P., Gudmundson, P., & Mikkelsen, L. P. (2009). Finite element implementation and numerical issues of strain gradient plasticity with application to metal matrix composites. *International Journal of Solids and Structures*, 46, 22-23, 3977-3987.
- Pan, B., Asundi, A., Xie, H., Gao, J. (2009). Digital image correlation using iterative least squares and pointwise least squares for displacement field and strain field measurements. *Optics and Lasers in Engineering*, 47,865–874.
- Pan, B., Qian, K., Xie, H., & Asundi, A. (2009). Two-dimensional Digital Image Correlation for in-plane displacement and measurement: A review, *Measure. Sci. Tech*., 20-6, 1-17.

- Pan, B., Wang, Z., &Xie, H. (2009). Generalized spatial-gradient based digital image correlation for displacement and shape measurement with subpixel accuracy. *The Journal of Strain Analysis for Engineering Design*, 44, 8. DOI:https://doi.org/10.1243%2F03093247JSA546
- Pan, B., Wang, Z., Xie, H., Guo, Z., & Tao Hua, T. (2007). Full-field strain measurement using a twodimensional Savitzky-Golay digital differentiator in digital image correlation, *Society of Photo-Optical Instrumentation Engineers.*
- Pan, B., Xie,H., Guo, Z., & Hua, T. (2007). Full-field strain measurement using a two-dimensional Savitzky-Golay digital differentiator in digital image correlation. *Optical Engineering*, 46(3), 033601.
- Polmear, I. J. (2004). Aluminium alloys—a century of age hardening. *In: Nie JF, Morton AJ, Muddle BC (eds) Materials forum, vol 28. Institute of Materials Engineering Australasia Limited, Melbourne, Australia.*
- Rana, R. S., Purohit, R., & Das, S. (2012). Reviews on the influences of alloying elements on the microstructure and mechanical properties of aluminium alloys and aluminium alloy composites. *International Journal of Scientific and Research Publications*, 2, 6, ISSN 2250-3153.
- Reu, P. (2014). All about speckles: aliasing. *Exp Tech,* 38(5):1–3 44.
- Reu, P. (2014). All about speckles: speckle size measurement. *Exp Tech* 38(6):1–2
- Reu, P. (2015). All about speckles: contrast. *Exp Tech,* 39(1):1–2
- Reu P (2015) All about speckles: edge sharpness. *Exp Tech,* 39(2): 1–2
- Reu, P. (2015). All about speckles: speckle density. *Exp Tech,* 39(3): 1–2
- Spitzig, W. A., Sober, R. J., & Richmond, O. (1975). Pressure dependence of yielding and associated volume expansion in tempered martensite. *Acta Metallurgica et Materialia*, 23, 885–893.
- Sutton, M. A., Orteu, J. J., Schreier, Hubert, (2009). Image Correlation for Shape, Motion and Deformation Measurements, Basic Concepts, Theory and Applications. ISBN 978-0-387-78747-3.
- Sutton, M. A., Wolters, W. J., Peters, W. H., Ranson, W. F., & McNeill, S. R. (1983). Determination of displacements using an improved digital correlation method, *Image and Vision Computing*. 1, 3, 133-139.
- Taylor, G. I., Quinney, H. (1932). The plastic distortion of metals. *Philosophical Transactions of the Royal Society*, A230, 323–352.
- Zhang, X., Qing-Suo, L. (2016). Influence of Alloying Element Addition on Cu–Al–Ni High Temperature Shape Memory Alloy without Second Phase Formation.*Acta Metallurgica Sinica, 29, 9, 884-888.*

Vipin Chandra *is a Ph.D. Scholar in the Department of Aerospace Engineering at IIT Kanpur. He has received his Master's degree in Aerospace Engineering from IIT Bombay in 2016. His research interests lie in the fields of solid mechanics, strain analysis using experimental and FEM simulation techniques, plasticity, facture and fatigue. He can be reached at chandrav@iitk.ac.in*

Pritam Chakraborty *is Assistant Professor in the Department of Aerospace Engineering at IIT Kanpur. He has done his Ph.D. in Mechanical Engineering from The Ohio State University and worked as a Scientist at Idaho National Laboratory, USA, before joining his current role. His interests are in solid mechanics, multi-scale modeling, fatigue, fracture, plasticity and large scale computing. He can be reached at cpritam@iitk.ac.in*